Cancer Science
Japanese Cancer Association JCA
Open Access

# Unusual prolongation of radiation-induced G2 arrest in tumor xenografts derived from HeLa cells

**Atsushi Kaida and Masahiko Miura**

Section of Oral Radiation Oncology, Department of Oral Health Science, Graduate School of Medical and Dental Sciences, Tokyo Medical and Dental University, Tokyo, Japan

**Key words**

Fluorescent ubiquitination-based cell cycle indicator (Fucci), G2 arrest, ionizing radiation, live imaging, tumor microenvironments

**Correspondence**

Masahiko Miura, Section of Oral Radiation Oncology, Department of Oral Health Science, Graduate School of Medical and Dental Sciences, Tokyo Medical and Dental University, 1-5-45 Yushima, Bunkyo-ku, Tokyo 113-8549, Japan.
Tel/Fax: +81-3-5803-5897;
E-mail: masa.mdth@tmd.ac.jp

**Funding Information**

Scientific Research from MEXT (26861569, 26293399, and 25670796).

Received March 18, 2015; Revised July 8, 2015; Accepted July 15, 2015

*Cancer Sci* **106** (2015) 1370–1376

doi: 10.1111/cas.12748

**The effect of ionizing radiation on cell cycle kinetics in solid tumors remains largely unknown because of technical limitations and these tumors' complicated structures. In this study, we analyzed intratumoral cell cycle kinetics after X-irradiation of tumor xenografts derived from HeLa cells expressing the fluorescent ubiquitination-based cell cycle indicator (Fucci), a novel system to visualize cell cycle kinetics *in vivo*. Cell cycle kinetics after X-irradiation was examined by using tumor sections and *in vivo* real-time imaging system in tumor xenografts derived from HeLa cells expressing Fucci. We found that G2 arrest was remarkably prolonged, up to 5 days after 10-Gy irradiation, in contrast to monolayer cultures where G2 arrest returned within 24 h. Cells isolated from tumors 5 days after irradiation exhibited a higher surviving fraction than those isolated immediately or one day after irradiation. In this study, we clearly demonstrated unusual post-irradiation cell cycle kinetics in tumor xenografts derived from HeLa-Fucci cells. Our findings imply that prolonged G2 arrest occurring in tumor microenvironments following irradiation may function as a radioresistance mechanism.**

Solid tumors have microenvironments characterized by hypoxia, lack of nutrients, and low pH.[1] Tumor cells often acquire therapeutic resistance in tumor microenvironments.[2,3] Formulating effective therapeutic strategies requires understanding the cell cycle kinetics that follow DNA damage in solid tumors where such environments are present; however, it has been difficult to obtain information on these kinetics due to limitations of techniques, such as flow cytometric analysis, which do not retain spatial information. Sakaue-Sawano *et al.*[4] developed a novel system, the fluorescent ubiquitination-based cell cycle indicator (Fucci), to visualize each cell cycle phase *in vivo*. This technique uses two proteins that originate from corals, monomeric Azami Green (mAG) and monomeric Kusabira Orange 2 (mKO2), which fluoresce *in vivo* during the S/G2/M and G1/G0 phases, respectively. Using this system, Yano *et al.*[5] reported that G1/G0-phase cells survived after treatment with ionizing radiation or cisplatin in spheroids and tumors with wild-type p53 because only growing cells were killed by the agents, but the kinetics of cell cycle arrest were not described in detail.

Ionizing radiation causes a variety of types of DNA damage in tumor cells, with double-strand breaks (DSB) being the most lethal.[6–9] It is well-known that many kinds of tumor cells lack functional p53, which accumulate in G2 phase due to DSB, leading to G2 arrest.[10,11] We previously visualized radiation-induced G2 arrest in live monolayer-cultured HeLa cells expressing Fucci (HeLa-Fucci cells).[12,13] We further described radiation-induced cell cycle kinetics in multi-cellular spheroids consisting of HeLa-Fucci cells as a tumor-like model.[14] Interestingly, the duration of radiation-induced G2 arrest in spheroids was significantly prolonged, and furthermore, cell cycle kinetics after irradiation differed between the outer and the inner spheroid layers. In this study, for the first time, we visualized unusual cell cycle kinetics after irradiation of tumor xenografts derived from HeLa-Fucci cells that were generated by tumor microenvironments. We further suggest that the unusual kinetics may provide a potential radioresistance mechanism.

## Materials and methods

**Cell line and culture conditions.** HeLa-Fucci cells were provided by the RIKEN BRC through the National Bio-Resource Project of MEXT, Japan. Cells were maintained in DMEM (Sigma-Aldrich, St. Louis, MO, USA) with 100 units/mL penicillin and 100 μg/mL streptomycin, supplemented with 10% fetal bovine serum, at 37°C in a 5% $CO_2$ humidified atmosphere.

**Xenograft establishment.** All animal experiments were approved by the Institutional Animal Care and Use Committee of Tokyo Medical and Dental University. HeLa-Fucci cells ($1 \times 10^7$ cells in 50 μL PBS) were implanted subcutaneously into the hind legs of male KSN nude mice (6 weeks old). Tumor xenografts took about a month to grow to the appropriate size (length of about 1 cm), at which point the mice

underwent the experiments described below and then were properly sacrificed. Tumor volume (V) was calculated using the following formula: $V = (\text{length} \times \text{width}^2)/2$.

**Irradiation.** Each xenograft tumor in non-anesthetized mice was irradiated with an HS-225 X-ray therapeutic machine (225 kVp, 15 mA, 1.0 mm Cu filtration: Shimadzu, Kyoto, Japan) at a dose rate of 0.9 Gy/min while shielding the body with lead.

**Optical imaging of mAG and mKO2 in tumor xenografts of HeLa-Fucci cells.** Before the imaging, mice were anesthetized with 40 mg/kg pentobarbital sodium in physiological saline. Optical imaging was performed with a Photon Imager (BIOSPACE LAB, Paris, France) to detect both mAG and mKO2. Acquired images were analyzed using M3Vision™ software (BIOSPACE LAB).

**Immunohistochemistry.** At each time point after irradiation, tumors were excised and fixed in 4% paraformaldehyde in PBS, then immersed in 20% sucrose in PBS until tumors sank to the bottom of the tube. Fixed tumors were embedded in OCT compound (Sakura, Tokyo, Japan) and stored at −80°C. For the detection of blood perfusion, 16 mg/kg Hoechst 33342 was injected intravenously 1 min before sacrifice. As a hypoxia marker, 60 mg/mL pimonidazole-HCl (Hypoxyprobe-1: Hypoxyprobe, Burlington, MA, USA) was injected intraperitoneally 30 min before sacrifice. Frozen and fixed tumors were cut by a cryostat into 10-μm sections. For detections of cyclin B1 and CENPF as G2 markers, tumor sections were boiled in HistoVT One solution (Nakalai Tesque, Kyoto, Japan) for at least 20 min at 90°C to retrieve the antigen. For the detection of pimonidazole, Target Retrieval Solution (Dako, Glostrup, Denmark) was applied and tumor sections were boiled for at least 20 min at 70°C. After the antigen retrieval treatment, non-specific antigens were blocked in Protein Block, Serum Free (Dako) for 10 min. Sections were incubated with anti-cyclin B1 antibody (clone: GNS1: Santa Cruz Biotechnology, Dallas, TX, USA), anti-CENPF (ab5: Abcam, Cambridge, UK), or anti-pimonidazole (Hypoxyprobe) for 60 min at room temperature; thereafter, Alexa Fluor 555 Goat Anti-Mouse IgG (H+L), Alexa Fluor 488 Goat Anti-Rabbit IgG (H+L), Alexa Fluor 647 Goat Anti-Mouse IgG (H+L), or Alexa Fluor 488 Goat Anti-Mouse IgG (H+L) (Molecular Probes, Eugene, OR, USA) was applied for 30 min at room temperature as the secondary antibody, respectively. After the immunoreaction, sections were mounted with ProLong Gold Antifade Reagent with DAPI (Molecular Probes). For detection of mAG/mKO2 and perfusion, neither the retrieval treatment nor the immunoreaction was performed, and sections were mounted only. Fluorescence images were obtained using a BIOREVO BZ-9000 fluorescence microscope (KEYENCE, Osaka, Japan). For the quantitative analysis, at least three regions in each section were randomly chosen and fluorescent areas were measured using ImageJ 1.44 software (available at http://rsbweb.nih.gov/ij/).

**Clonogenic survival assay.** To assess the effect of prolonged *in vivo* G2 arrest on cell survival, tumors were excised immediately after sacrifice at specific times after 10-Gy irradiation. Excised tumors were minced using scalpels and disaggregated by collagenase and trypsin for preparation of single cell suspensions. Equal number of isolated single cells were plated on dishes and incubated for about 10 days. Colonies were fixed and stained with crystal violet. Colonies consisting of more than 50 cells were counted and surviving fractions (SF) were calculated as follows:

$$\text{SF} = [\text{number of colonies}/\text{number of irradiated cells plated}]/[(\text{number of colonies}/\text{number of non-irradiated cells plated})].$$

**Statistical analysis.** Mean values were statistically compared using the two-tailed t-test. $P$-values $< 0.05$ were considered statistically significant.

## Results

**Characterization of tumor xenografts derived from HeLa-Fucci cells.** We established tumor xenografts derived from HeLa-Fucci cells and analyzed the expression of mAG and mKO2 in tumor sections. There was no specific localization of mAG or mKO2 in peripheral or perinecrotic regions; however, expression of mKO2 was higher than that of mAG throughout the tumor sections (Fig. 1a). By injecting Hoechst 33342 immediately before sacrifice, perfused blood vessels were visualized in tumor sections (Fig. 1b), where expression of mKO2 was also higher than that of mAG. Interestingly, perinecrotic regions contained areas in which Fucci fluorescence was negative and only DAPI staining was positive (designated DAPI (+) areas) (Fig. 1c). To examine the relationship between DAPI (+) areas and hypoxic fractions, pimonidazole was administered as a hypoxic marker.[15] DAPI (+) areas were not stained with pimonidazole. Hypoxic fractions were observed outside of DAPI (+) areas, where mKO2 was more highly expressed (Fig. 1d). It was speculated that DAPI (+) areas consisted of death-committed cells that had lost most biochemical activity. Taken together, mKO2 expression was predominant in tumor xenografts that had not been irradiated. Perinecrotic regions were hypoxic, but there was no characteristic difference in fluorescence distribution between oxic and hypoxic areas.

**Fluorescence kinetics in tumor xenografts of HeLa-Fucci cells after irradiation.** To characterize cell cycle kinetics following irradiation of tumor xenografts, we analyzed fluorescence distributions in tumor sections at varying times after 10-Gy irradiation (Fig. 2a). Interestingly, a remarkable change was observed on Day 1 after irradiation compared to Day 0: peripheral areas were green, whereas perinecrotic ones were red (Fig. 2a: Day 1). Furthermore, most cells in all areas, including perinecrotic regions, became green 2 days after irradiation. This green-dominant state persisted for at least 5 days (Fig. 2a,b). As a reference, the fluorescence kinetics in monolayer cultures are shown in Supplementary Figure S1.

The fluorescence intensities of both mAG and mKO2 could be quantitated in live mice (Suppl. Fig. S2a). The fluorescence intensity ratio of mAG to mKO2 (mAG/mKO2) was similar to that in tumor sections (Suppl. Fig. S2b,c). Next, we analyzed fluorescence kinetics after irradiation in live nude mice bearing tumor xenografts (Fig. 2c). In non-irradiated tumor xenografts (0 Gy), the fluorescence of both mAG and mKO2 was always detectable and the mAG/mKO2 fluorescence ratio was <1 (Fig. 2d: 0 Gy). Following 10-Gy irradiation, the ratio increased dramatically and peaked around 2 days after irradiation. The predominance of green fluorescence persisted for more than 5 days in live mice bearing tumor xenografts as well as in tumor sections. Fluorescence kinetics showed a similar tendency in independent experiments albeit with slight differences in the peak time (Suppl. Fig. S3). The reason why the values in Figure 2(d) are enhanced compared to those in Figure 2(b) is due to Fucci properties; the promoter activity in

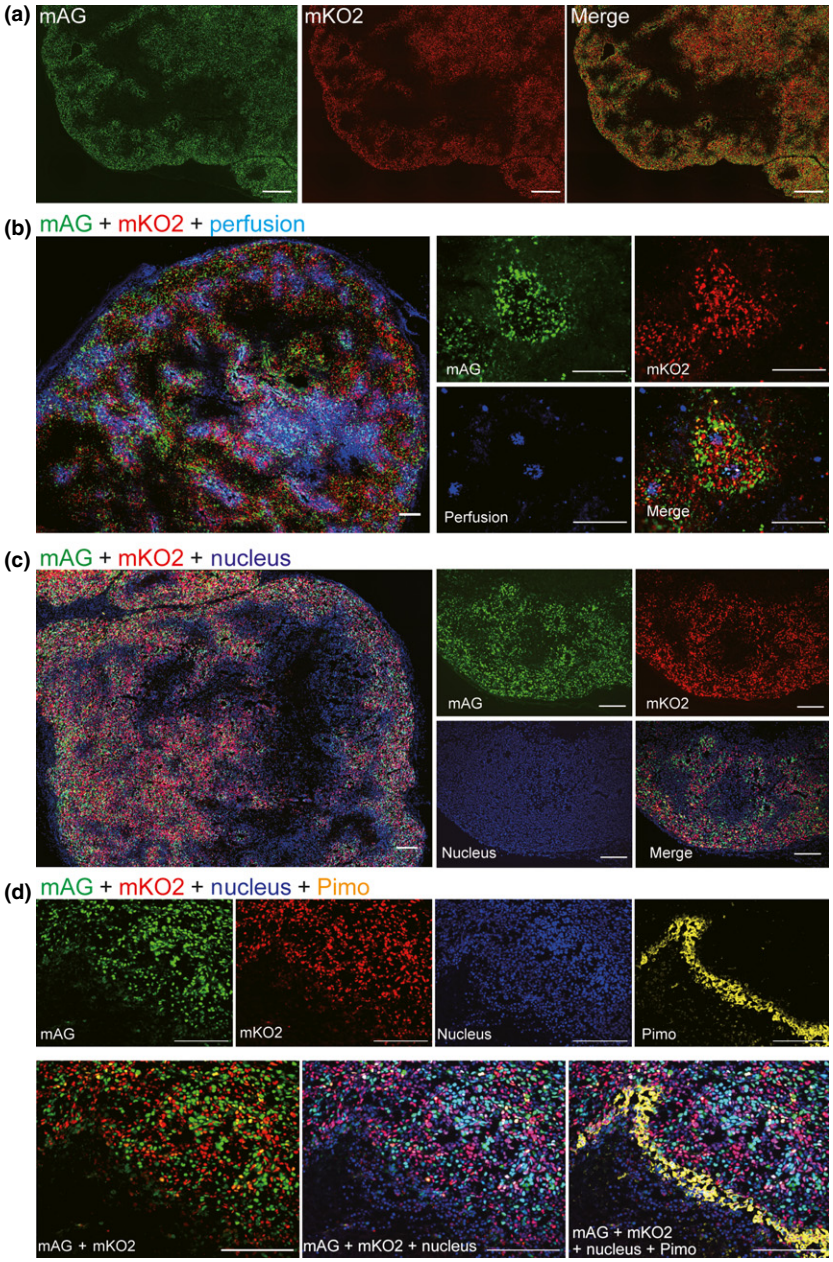


**Fig. 1.** Characterization of tumor xenografts originating from HeLa-Fucci cells. (a) Fluorescence images of tumor xenograft sections. Bar: 500 μm. (b and c) Fluorescence images of tumor xenograft sections. Low magnification images of mAG and mKO2 are merged with images of perfused vessels and nuclei, respectively. Bar: 500 μm. High magnification images are composed of each staining and a merged one. Bar: 200 μm. (d) Localization of a hypoxic maker (Hypoxyprobe-1: Pimo) in sections of tumor xenografts. Bar: 200 μm. Data are representative of four independent experiments.

Fucci probes is constitutively active, and therefore, intensity of green fluorescence remarkably increases when cells stop at G2 phase for a long time.

**Verification of G2 arrest in tumor xenografts after irradiation.** Previous studies on cell cycle kinetics in monolayer cultures[12,13] strongly suggested that the green-dominant state in irradiated tumor xenografts represented prolongation of radiation-induced G2 arrest. To verify this, we examined the expression of cyclin B1 and CENPF as G2 phase markers.[16,17] In tumor sections 5 days after irradiation, most green cells expressed cyclin B1 in the cytoplasm and CENPF in the nucleus (Fig. 3a,c). Furthermore, quantitative analysis of both proteins supported the above hypothesis (Fig. 3b,d).

**Potential contribution of prolonged G2 arrest to radioresistance in xenografted tumors.** We previously reported that the release from radiation-induced G2 arrest was accelerated by attaching spheroids to the bottom of the culture dish.[14] G2-arrested cells isolated from a tumor xenograft one day or 5 days after irradiation were more rapidly released from G2 arrest when attached to a culture dish (Fig. 4a, Suppl. Fig. S4) than cells in an *in vivo* condition (Fig. 2). This rapid release from prolonged G2 arrest prompted us to consider the possibility of induction of radiosensitization. We therefore examined cell survival in tumor cells isolated from tumor xenografts at various times after irradiation (Fig. 4b). The surviving fraction significantly increased in isolated tumor cells 5 days after irradiation, compared to those isolated immediately or one day after irradiation (Fig. 4c). The trypan blue exclusion test showed that cell viability of isolated tumor cells was similar between non-irradiated tumors and tumors one day or five days after irradiation, and there were no significant changes (Control: 63.67% ± 12.4%; Day 1: 52.9% ± 5.4%; Day 5: 55.1% ± 15.7%). Also, the mean tumor volume on Day 6 decreased to 90.5% ± 10.5% of that before irradiation, but

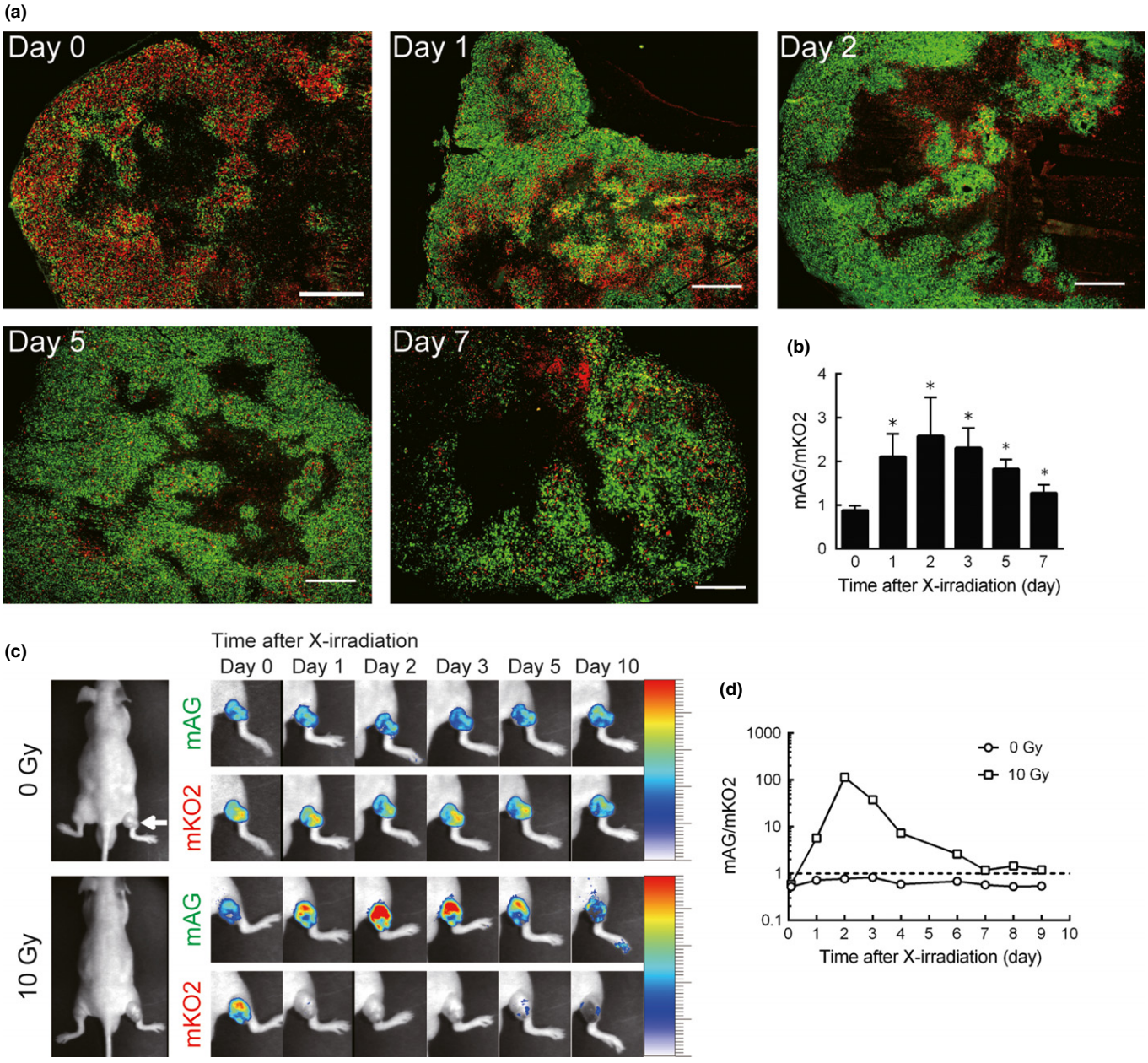


**Fig. 2.** Fluorescence kinetics in tumor xenografts after 10-Gy irradiation. (a) Fluorescence images of tumor sections at the indicated times after 10-Gy irradiation. Data are representative of at least four independent experiments. Bar: 500 μm. (b) The ratio of mAG-positive to mKO2-positive areas (mAG/mKO2) in tumor sections at the indicated times after 10-Gy irradiation. mAG/mKO2 was calculated by dividing the mAG-positive area by the mKO2-positive area and is plotted as a function of time after irradiation. Data are means ± SD in three independent fields. *$P$ <0.05 vs. Day 0. (c) Optical imaging of mAG and mKO2 at the indicated times after 0- or 10-Gy irradiation in live mice bearing tumor xenografts. (d) The ratio of green fluorescence intensity to red fluorescence intensity (mAG/mKO2) in live nude mice bearing tumor xenografts after 0- or 10-Gy irradiation. mAG/mKO2 was calculated by dividing photon counts of green fluorescence by those of red fluorescence and is plotted as a function of time after irradiation. Data shown in (c) and (d) are representative of three independent experiments.

this difference was not significant. Thus, we speculate that the increase in the surviving fraction on Day 5 was not an artifact of cell loss at the early time. Taken together, we reasoned that the prolonged G2 arrest served *in vivo* after irradiation is likely to contribute to a potential radioresistance mechanism.

## Discussion

In this study, we demonstrated the following novel findings regarding tumor xenografts derived from HeLa-Fucci cells after irradiation: (i) remarkable prolongation, up to 5 days, of the green phase, representing radiation-induced G2 arrest; (ii) two distinct red (in the perinecrotic region) and green (in the peripheral region) fluorescent regions observed 24 h after irradiation; (iii) transition from red to green fluorescence two days after irradiation; and (iv) enhanced cell survival during the elongated G2 arrest.

The fluorescence kinetics are reminiscent of those we previously observed in spheroids,[14] although there was more significant prolongation of G2 arrest in solid tumors. In 500-μm-diameter spheroids consisting of HeLa-Fucci cells, there was no significant difference in the distribution of either red or green

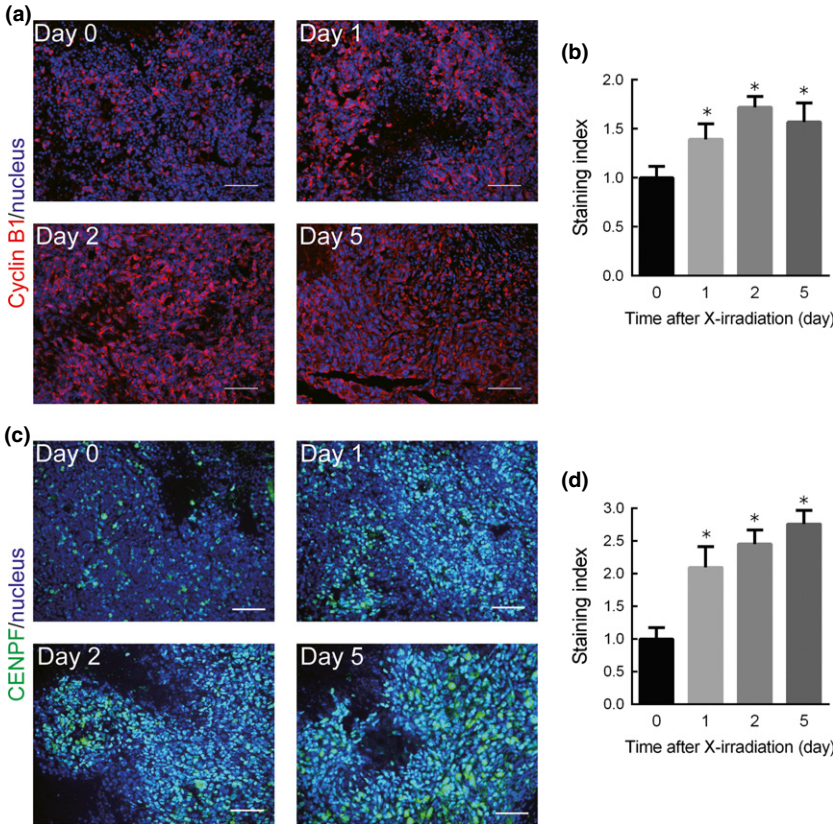


**Fig. 3.** Expression of cyclin B1 and CENPF as markers of G2 phase in tumor sections following irradiation. (a and c) Immunohistochemical staining of cyclin B1 and CENPF, respectively, in tumor sections at the indicated times after 10-Gy irradiation. Bar: 100 μm. Data are representative of at least four independent fields. (b and d) The ratio of the cyclin B1- or CENPF-positive area to the nuclei-positive area in tumor sections at the indicated times after 10-Gy irradiation. Staining index was calculated by dividing the cyclin B1- or CENPF-positive area by the nuclei-positive area and is expressed normalized to the staining index on Day 0. Data are means ± SD in three independent fields. **P* <0.05 vs. Day 0.

fluorescence, though red was somewhat predominant between the outer and inner layers.[4] The outer layer, with a thickness of approximately 100 μm, became green 16 h after irradiation, while the inner region remained red. Interestingly, following irradiation the green phase persisted in the outer layer of spheroids for more than 48 h longer than in monolayer cultures. The inner region began turning green 24 h after irradiation and remained green for as long as 48 h, suggesting recruitment from the quiescent to the growing phase. Judging from the structural homology between spheroids and solid tumors, the outer and inner regions correspond to the peripheral and perinecrotic areas of solid tumors, respectively. However, the elongation of G2 arrest was somehow remarkably enhanced in solid tumors (Fig. 2), which may have resulted both from complicated structures and the degree of tumor microenvironments. The spheroids used in the study had diameters of approximately 500 μm with no internal necrosis[14] while the solid tumors used in this study had diameters of approximately 1 cm and were characterized by internal necrosis and vasculature. It is well-established that the tumor microenvironment is acidic.[1] Park *et al.*[18] reported that compared to pH 7.5 medium, pH 6.6 medium demonstrated enhanced radiation-induced G2 arrest and induction of radioresistance. Although we do not have data regarding pH in spheroids and solid tumors, it is quite interesting to consider the possibility that a disparity in pH may explain the differences between the two in terms of elongation of radiation-induced G2 arrest. Further study will be necessary to elucidate this issue.

Double-strand breaks repair kinetics closely correlate with cell cycle kinetics following irradiation, particularly the release from G2 arrest. Indeed, many DSB remain in tumor xenografts for an extended period of time (Suppl. Fig. S5), whereas DSB repair is completed soon after irradiation in monolayer cultures (data not shown). Namely, it is conceivable that DSB repair rate seems to be somehow reduced in tumor microenvironments, leading to a prolonged G2 arrest *in vivo*. Chan *et al.*[19] revealed that DSB repair was suppressed under chronic hypoxia due to the low expression of several homologous recombination (HR) proteins, resulting in an oxygen enhancement ratio (OER) of 1.37 compared to 1.96–2.61 under acute hypoxia. In our study, however, prolongation of G2 arrest occurred not only in severe hypoxic fractions, but also in peripheral regions (Fig. 2a); therefore, suppression of DSB repair cannot be explained by hypoxia alone. It has also been reported that DSB repair is affected by other tumor microenvironmental factors, such as acidic conditions and extracellular matrix expression.[18–21] Further study is needed to elucidate the detailed mechanism.

We next considered how the unusually prolonged G2 arrest observed in this study influenced radiosensitivity. Although a slow DSB repair rate is generally thought to be a disadvantage in cell survival, cells remaining in G2 phase for a long time demonstrated a higher surviving fraction than those isolated immediately after irradiation (Fig. 4c). Thus, prolongation of G2 arrest is likely to be advantageous in tumor-cell survival. As in this study, previous reports performed colony formation assays on cells isolated from xenografted tumors at various times after irradiation.[22,23] The surviving fractions of tumor cells isolated several hours after irradiation were larger than those of cells isolated immediately after irradiation, which is a well-known result of potentially lethal damage repair (PLDR). This phenomenon is mainly associated with the non-homologous end-joining (NHEJ) pathway due to DSB repair of quiescent solid tumor cells at the G0 phase. Our findings are inconsistent with previous studies in that we observed recovery of cell survival during G2 arrest, not G1/G0 phase. A recent study demonstrated PLDR in G2 phase, where the HR pathway

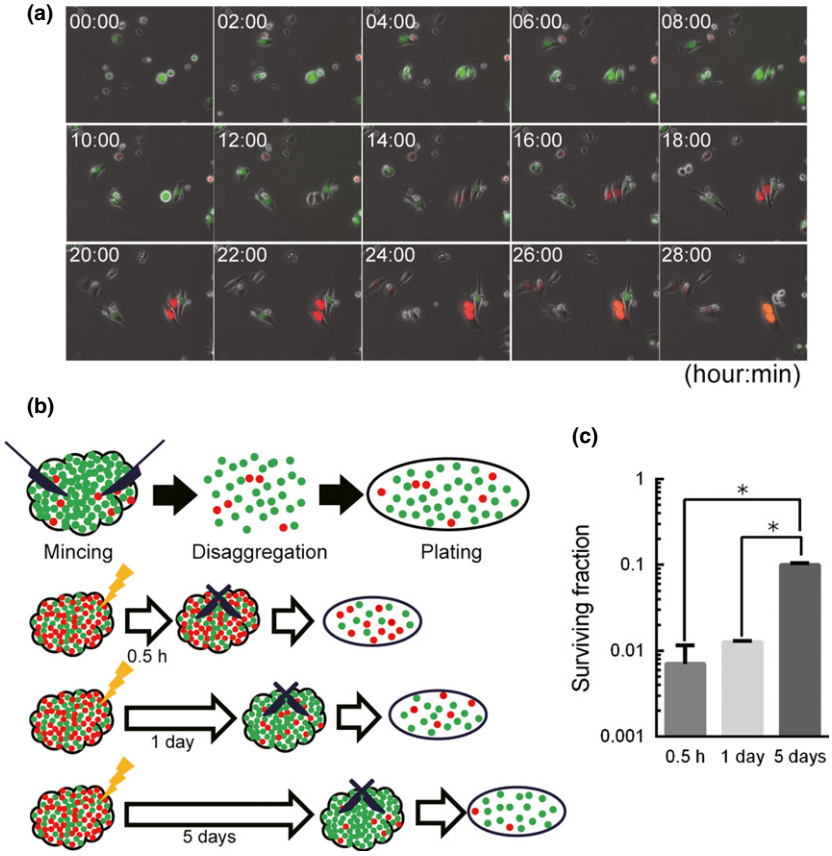


**Fig. 4.** Effect on cell survival of prolonged G2 arrest observed *in vivo* following irradiation (a) Fluorescence kinetics of HeLa-Fucci cells isolated from a tumor xenograft following irradiation. The tumor xenograft was excised one day after 10-Gy irradiation and a single cell suspension was prepared for time-lapse imaging. (b) Schematic presentation of experimental design to assess survival of tumor cells isolated from tumor xenografts following irradiation. Tumor xenografts were irradiated at a dose of 10 Gy and single cell suspensions were prepared for clonogenic assay. Red and green represent Fucci fluorescence, reflecting G2 arrest kinetics following irradiation. (c) Surviving fractions of tumor cells isolated from tumor xenografts at the indicated times after 10-Gy irradiation. Data are means ± SD from three independent experiments. *$P$ <0.05.

plays a critical role.[24] It is still unclear whether the same mechanism also occurs in the very slow PLDR during the prolonged G2 arrest *in vivo*. Nevertheless, two plausible radiosensitizing strategies could be used in the context of such a radioresistance mechanism. One is fractionated stereotactic radiotherapy using more than 10 Gy per fraction and total treatment duration within 1 week. In this regimen, prolonged G2 arrest provides quite an efficient redistribution of the cell cycle toward the radiosensitive G2/M boundary. Another approach might be to release cells from elongated G2 arrest using Chk1 or Wee1 inhibitors, which demonstrate G2/M checkpoint inhibition, resulting in enhanced radiosensitization.

In this study, we demonstrated that radiation-induced G2 arrest was remarkably prolonged in tumor xenografts derived from HeLa-Fucci cells, which seemed to be attributed to enhanced cell survival. Because HeLa-Fucci cells do not show G1 arrest after irradiation due to p53 deficiency, further studies will be needed in order to verify whether this phenomenon occurs only in p53-deficient cells or not. Understanding radiation-induced cell cycle kinetics in solid tumors is important to formulate the effective therapeutic strategies. This study will provide supportive information as a valuable piece of evidence that tumor microenvironments affects cell cycle kinetics and cell survival in irradiated solid tumors.

## Acknowledgements

The authors thank Dr. A. Miyawaki and Dr. A. Sakaue-Sawano for providing the HeLa cells expressing the Fucci probes. This study was supported in part by Grants-in-Aid for Scientific Research from MEXT (26861569, 26293399, and 25670796) to A.K. and M.M.

## Disclosure Statement

The authors do not have any conflicts of interest.

## References

1 Hanahan D, Weinberg RA. Hallmarks of cancer: the next generation. *Cell* 2011; **144**: 646–74.
2 Harada H, Inoue M, Itasaka S *et al.* Cancer cells that survive radiation therapy acquire HIF-1 activity and translocate towards tumour blood vessels. *Nat Commun* 2012; **3**: 783.
3 Meijer TW, Kaanders JH, Span PN, Bussink J. Targeting hypoxia, HIF-1, and tumor glucose metabolism to improve radiotherapy efficacy. *Clin Cancer Res* 2012; **18**: 5585–94.
4 Sakaue-Sawano A, Kurokawa H, Morimura T *et al.* Visualizing spatiotemporal dynamics of multicellular cell-cycle progression. *Cell* 2008; **132**: 487–98.
5 Yano S, Tazawa H, Hashimoto Y *et al.* A genetically engineered oncolytic adenovirus decoys and lethally traps quiescent cancer stem-like cells in S /G2/M phases. *Clin Cancer Res* 2013; **19**: 6495–505.
6 Jackson SP, Bartek J. The DNA-damage response in human biology and disease. *Nature* 2009; **461**: 1071–8.
7 Wang C, Lees-Miller SP. Detection and repair of ionizing radiation-induced DNA double strand breaks: new developments in nonhomologous end joining. *Int J Radiat Oncol Biol Phys* 2013; **86**: 440–9.
8 Valerie K, Povirk LF. Regulation and mechanisms of mammalian double-strand break repair. *Oncogene* 2003; **22**: 5792–812.
9 Khanna KK, Jackson SP. DNA double-strand breaks: signaling, repair and the cancer connection. *Nat Genet* 2001; **27**: 247–54.
10 Pellegata NS, Antoniono RJ, Redpath JL, Stanbridge EJ. DNA damage and p53-mediated cell cycle arrest: a reevaluation. *Proc Natl Acad Sci U S A* 1996; **93**: 15209–14.
11 Löbrich M, Jeggo PA. The impact of a negligent G2/M checkpoint on genomic instability and cancer induction. *Nat Rev Cancer* 2007; **7**: 861–9.

12 Kaida A, Sawai N, Sakaguchi K, Miura M. Fluorescence kinetics in HeLa cells after treatment with cell cycle arrest inducers visualized with Fucci (fluorescent ubiquitination-based cell cycle indicator). *Cell Biol Int* 2011; **35**: 359–63.
13 Kaida A, Miura M. Visualizing the effect of hypoxia on fluorescence kinetics in living HeLa cells using the fluorescent ubiquitination-based cell cycle indicator (Fucci). *Exp Cell Res* 2012; **318**: 288–97.
14 Kaida A, Miura M. Visualizing the effect of tumor microenvironments on radiation-induced cell kinetics in multicellular spheroids consisting of HeLa cells. *Biochem Biophys Res Commun* 2013; **439**: 453–8.
15 He F, Deng X, Wen B *et al.* Noninvasive molecular imaging of hypoxia in human xenografts: comparing hypoxia-induced gene expression with endogenous and exogenous hypoxia markers. *Cancer Res* 2008; **68**: 8597–606.
16 Theron T, Böhm L. Cyclin B1 expression in response to abrogation of the radiation-induced G2/M block in HeLa cells. *Cell Prolif* 1998; **31**: 49–57.
17 Liao H, Winkfein RJ, Mack G, Rattner JB, Yen TJ. CENP-F is a protein of the nuclear matrix that assembles onto kinetochores at late G2 and is rapidly degraded after mitosis. *J Cell Biol* 1995; **130**: 507–18.
18 Park HJ, Lee SH, Chung H *et al.* Influence of environmental pH on G2-phase arrest caused by ionizing radiation. *Radiat Res* 2003; **159**: 86–93.
19 Chan N, Koritzinsky M, Zhao H *et al.* Chronic hypoxia decreases synthesis of homologous recombination proteins to offset chemoresistance and radioresistance. *Cancer Res* 2008; **68**: 605–14.
20 Okada S, Ono K, Hamada N, Inada T, Kubota N. A low-pH culture condition enhances the radiosensitizing effect of wortmannin. *Int J Radiat Oncol Biol Phys* 2001; **49**: 1149–56.
21 Ponnala S, Veeravalli KK, Chetty C, Dinh DH, Rao JS. Regulation of DNA repair mechanism in human glioma xenograft cells both *in vitro* and *in vivo* in nude mice. *PLoS ONE* 2011; **6**: e26191.
22 Hall EJ, Giaccia J. Fractionated radiation and the dose-rate effect. In: Hall EJ, Giaccia J, eds. *Radiobiology for the Radiologist*, 7th edn. Philadelphia: Lippincott Williams & Wilkins, 2012; 67–85.
23 Little JB, Hahn GM, Frindel E, Tubiana M. Repair of potentially lethal radiation damage *in vitro* and *in vivo*. *Radiology* 1973; **106**: 689–94.
24 Maeda J, Bell JJ, Genet SC *et al.* Potentially lethal damage repair in drug arrested G2-phase cells after radiation exposure. *Radiat Res* 2014; **182**: 448–57.

## Supporting Information

Additional supporting information may be found in the online version of this article:

**Data S1**. Supporting Materials and Methods

**Fig. S1**. Fluorescence kinetics after 10-Gy irradiation of monolayer cultures.

**Fig. S2.** Detection of mAG and mKO2 in live nude mice bearing tumor xenografts.

**Fig. S3**. Values of mAG/mKO2 over time in other live mice bearing tumor xenografts after 10-Gy irradiation.

**Fig. S4**. Fluorescence kinetics of HeLa-Fucci cells isolated from a tumor xenograft following irradiation.

**Fig. S5.** Nuclear formation of γH2A.X foci in tumor sections before and after 10-Gy irradiation.